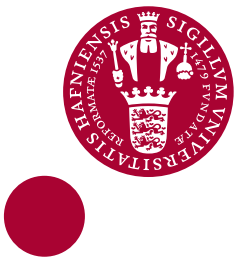

Neutron guide shielding for the BIFROST spectrometer at ESS

Mantulnikovs, Konstantins; Bertelsen, Mads; Cooper-jensen, C.p.; Lefmann, Kim; Klinkby, Esben Bryndt

Published in:
Journal of Physics - Conference Series

DOI:
10.1088/1742-6596/746/1/012027

Publication date:
2016

Document version
Publisher's PDF, also known as Version of record

Neutron guide shielding for the BIFROST spectrometer at ESS

2016 J. Phys.: Conf. Ser. 746 012027

(http://iopscience.iop.org/1742-6596/746/1/012027)

Neutron guide shielding for the BIFROST spectrometer at ESS

K. Mantulnikovs[1], M. Bertelsen[1], C.P. Cooper-Jensen[2,3], K. Lefmann[1] and E.B. Klinkby[3,4]

[1] Nano-Science Center, Niels Bohr Institute, University of Copenhagen, Denmark
[2] Department of Physics and Astronomy, Uppsala University, Uppsala, Sweden
[3] European Spallation Source ESS AB, Lund, Sweden
[4] Center for Nuclear Technologies, Technical University of Denmark, Denmark

E-mail: esbe@dtu.dk

Abstract. We report on the study of fast-neutron background for the BIFROST spectrometer at ESS. We investigate the effect of background radiation induced by the interaction of fast neutrons from the source with the material of the neutron guide and devise a reasonable fast, thermal/cold neutron shielding solution for the current guide geometry using McStas and MCNPX. We investigate the effectiveness of the steel shielding around the guide by running simulations with three different steel thicknesses. The same approach is used to study the efficiencies of the steel wall a flat cylinder pierced by the guide in the middle and the polyethylene layer. The final model presented here has a 3 cm thick steel shielding around the guide, 30 cm of polyethylene around the shielding, two 5 mm thick B_4C layers and a steel wall at position Z = 38 m, being 1 m thick and 10 m in radius. The final model finally proves that it is sufficient to bring the background level below the cosmic neutron rate, which defines an order of magnitude of the lowest obtainable background in the instruments.

1. Introduction

The worlds strongest neutron source for the study of materials and biosystems will be the European Spallation Source (ESS) [1], which is presently under construction in Lund, Sweden. At ESS, neutrons will be produced by a 2 GeV protons impinging on a rotating tungsten target. The beam power will reach 5 MW resulting in unprecedented cold and thermal neutron brightness, but will also give rise to experimental backgrounds to a level beyond what is observed at existing neutron facilities [2].

Prompt neutrons escaping the target monolith have energies reaching up to the energy of the initial proton beam, and thus the task of instrument shielding is completely different compared to the case of reactor sources, based on which most shielding experience relies. At neutron energies exceeding 10 MeV, the scattering cross section of most commonly used shielding materials drops dramatically meaning that the task of instrument shielding at the ESS is even more complex than what the proton beam power dictates.

Having in mind also that ultimately the performance of most instruments mostly depends on the signal-to-noise ratio (S/N), and that shielding is expected to be a significant cost driver of the facility, the shielding design at ESS is as important as it is complex.

The present study focusses on evaluating the shielding options of the BIFROST spectrometer, which will in 2016 enter Phase 1 of its technical design at ESS. The beam optics of BIFROST is designed and optimised using the ray-tracing code McStas [3, 4, 5, 6, 7]. While McStas is well-recognised for its capability to precisely describe neutron scattering instruments in terms of signal distributions, it does lack in the description of backgrounds. To remedy this challenge an exact one-to-one implementation of the instrument is developed MCNPX [8, 9] - which is the standard Monte Carlo tool used for shielding calculations. Below we study the performance of various shielding design options considered for the BIFROST instrument. The aim of such study is to outline the shielding design prior to the instrument construction, hereby allowing to iterate the instrument and shielding design to a common optimum.

2. Methods

MCNP and MCNPX are general purpose Monte Carlo radiation transport codes that have the ability to track many particle types over a broad energy range. These capabilities include but are not limited to tracking protons and electrons. MCNP and MCNPX stands for Monte Carlo N-Particle and Monte Carlo N-Particle Extended. The extended version has been developed to simulate 34 different particle types and more than 2000 heavy ions in a broad range of energies.

McStas is a ray tracing software package for simulating neutron scattering experiments from the moderator to the detector. Such experiments can be described by a series of components, where the ray is propagated through each one without the ability to move back, which enables the code to be relatively simple, fast and modular. For this reason, McStas is well suited to exploration of possibilities, as development times are manageable, and the resulting simulations are fast enough to be used with numerical optimisers.

When designing a neutron guide system, there is a overwhelming amount of possibilities, even when only considering the geometry of the guide system. Writing McStas code for every possibility is unfeasible for a single person designing a neutron instrument, meaning that a small number of possible solutions can be investigated. The program guide_bot [10] is meant to reduce the time spent coding in these initial stages of project design, as it will write McStas guide optimisations tailored to the specific requirements of the instrument from a very limited amount of user input. The optimised guides are then automatically compared with comprehensive performance analysis for each case, making the decision making in neutron guide design more informed.

This project also makes use of the McStas-MCNPX coupling interface [11, 12], which takes advantage of the specific areas of expertise of each software package. More precisely, this coupling is used due to the fact that there are no models in MCNPX that account for reflectivity of the neutron guide – this is the area where one would need to use McStas, which is made to perform ray-tracing simulation of neutron transport in the neutron guides.

Since MCNPX and McStas are both Monte Carlo based software packages one would need significant computer power to run simulations on. In this project the cluster of the ESS Science division based in Data Management and Software Centre (DMSC) in Copenhagen is used. The cluster consists of the following components [13]:

- 42 compute nodes, each consisting of 2 processors (Intel Xeon 2.66 GHz) with 6 cores each and 48 Gb memory;
- 50 Tb of storage;
- Management network, used for maintenance;
- InfiniBand network, connecting the nodes in between each other as well as connecting them with the storage system;
- A batch-system for handling jobs.

3. Model description

The BIFROST spectrometer [14, 15] was accepted for construction in 2014 and is designed to achieve high detection efficiency in the horizontal scattering plane. Apart from the spectrometer

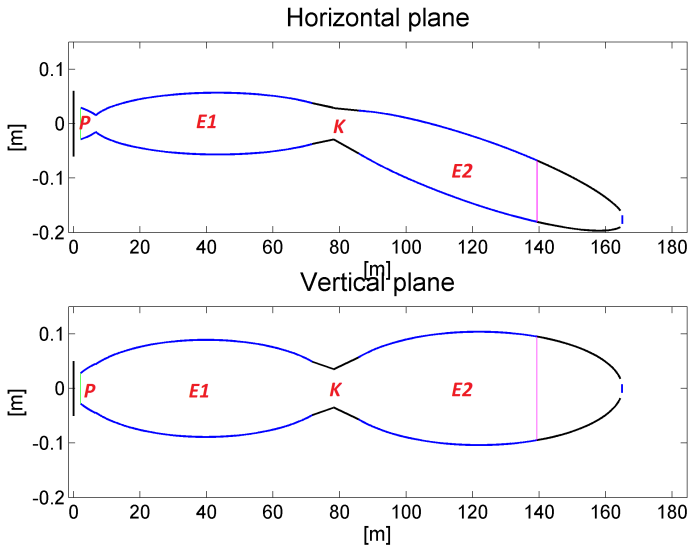

Figure 1. ZX (top) and ZY (bottom) cross sections of the BIFROST neutron guide obtained from McStas. The direction of the guide (the direction of the guide's optical axis) is along the Z axis, the X axis is represented in top image, Y axis – in the bottom one. The guide is composed out of four main sections: P – parabolic feeder, E1 and E2 – two elliptic sections that are connected by the kink – K. Parabolic and elliptic shapes are used to improve neutron intake and transport to the sample, while at the kink the guide's second elliptic section E2 is rotated out of line-of-sight (line-of-sight is broken at the magenta line) to avoid direct beam from the moderator.

itself BIFROST has a neutron guide – a tube that is used to transport cold neutrons to the sample position. The direction of the guide is along the Z axis with the Y axis pointing upwards and X to the right, forming a left-handed coordinate system. The guide, seen in figure 1 utilizes a parabolic feeder to improve neutron intake as well as to decrease the parasitic background [16]. The following neutron guide sections are shaped as a double ellipses to improve neutron transport to the sample position and the optical axis has a kink between the two ellipses to avoid line-of-sight. To take advantage of the time-of-flight measurement technique BIFROST's neutron guide is a long guide with length of 162.24 m and the sample position is situated 164.24 m away from the moderator.

The MCNPX model is based on MIRROTRON's metal-glass sandwich technology [17] with a slight alteration. The world outside the guide is represented by a box, filled with air ($\rho = 1.296 \cdot 10^{-3}$ g/cm^3), spanning ± 100 m in the X and Y directions and 164.41 m along Z.

The model used in this study uses the combination of the conventional shielding measures such as steel and polyethylene along with the boron carbide (B_4C) as well as has a steel wall, which mimics the steel end wall of the planned shielding bunker. The modelled wall is basically a flat disk pierced by the guide in the middle. The reasoning for placing a steel wall is that high energy neutrons can get past the initial monolith and guide shielding due to presence of windows (minima) in the cross section. Fast neutrons having energies within windows would then travel

far away from the source and increase the background locally [18]. The steel wall is expected to stop these stray neutrons close to the monolith shielding and prevent their propagation closer to the sample position. The material stack-up in the guide in XY cross section is as follows and can be seen in figure 2:

- 2 μm thick Ni/Ti coating ($\rho = 6.45$ g/cm^3), which serves as a supermirror;
- 1 cm thick substrate of variable material, serving as a structure material;
- 1, 2 or 3 cm thick stainless steel shielding ($\rho = 8.03$ g/cm^3) around the guide;
- 20, 30 or 40 cm thick polyethylene (PE) layer ($\rho = 0.97$ g/cm^3) around the guide to moderate and scatter fast neutrons;
- Two 5 mm thick B_4C layers: one, around the steel shielding (only last 10 m of the guide) and another around the polyethylene to absorb neutrons moderated by the PE layer.

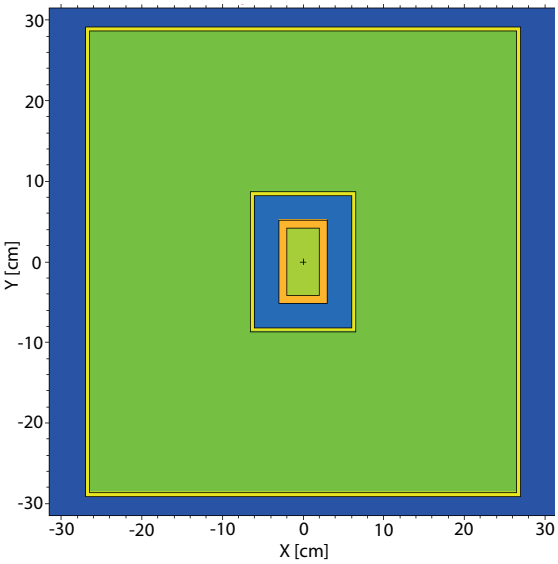

Figure 2. XY cross sections of the final model for BIFROST spectrometer's neutron guide shielding. The inner green is the guide vacuum (low pressure helium atmosphere) inside the Ni/Ti supermirror coating, which is supported by the substrate (yellow frame around the vacuum). The substrate is covered with stainless steel (cyan), serving as initial shielding. The thin yellow frame around steel is the boron carbide layer, which is present only in the last 10 m of the guide. Next layer is the PE layer – a conventional material to moderate fast neutrons and finally the same thin yellow frame of boron carbide to absorb the moderated neutrons. The outside (dark blue) is air.

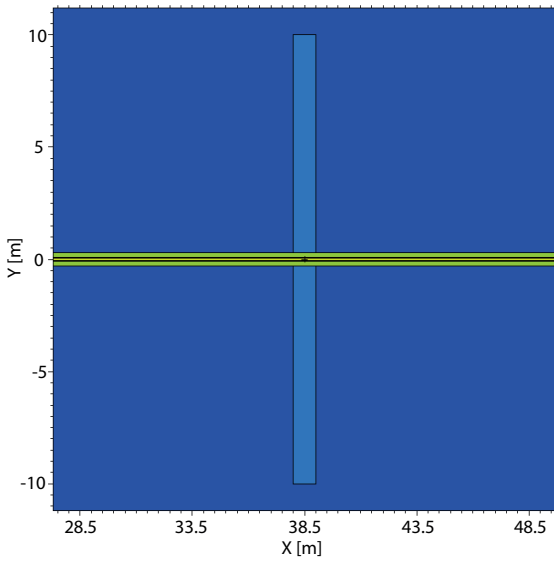

Figure 3. ZX cross sections of the final model for BIFROST spectrometer's neutron guide shielding explicitly showing the steel wall. The outside of the guide (dark blue) is air and the shield is depicted in cyan. It has a 10 m radius and 1 m thickness, being placed at position Z = 38 m.

The variable material of the guide's substrate changes depending on the position along the guide. First 20 m there is a copper substrate ($\rho = 8.96$ g/cm^3), the next 58 m the material is

aluminium ($\rho = 2.73$ g/cm^3) and then until the end of the guide – BORKRON glass ($\rho = 2.39$ g/cm^3). Note that parallel to the work described in this paper it has been shown that the sections made of copper and aluminium are going to be much shorter and the distance previously covered by copper or aluminium sections will be made out of glass. Apart from the lateral stack described above there is a stainless steel wall, seen in figure 3, with radius of 10 m and 0.5, 1 or 2 m thickness for further shielding of fast neutrons placed at position Z = 38 m. This is just before the place where the first elliptic section of the guide is the thickest, thus placing the shield here we expect neutrons to see less material with which they can interact and consequently bring the background level up.

The monolith shielding is made as a steel cylinder with wall thickness of approximately 3.3 m and is centred around the centre of the moderator, which is at Z = 15.54 cm. The choice of the wall thickness is mostly arbitrary but has the idea that even when the construction of the monolith shielding is unknown, we want to study the effect of neutrons entering the guide rather then focusing on the monolith shielding. Thus the walls have been chosen to be thick enough to stop most of the neutrons that come from the source but do not end up in the guide opening.

The MCNPX detectors are placed in two positions. First, just before the kink (Z = 71.8 m), before the guide have turned and the model is symmetric with respect to the origin, so that the data acquired at this position are easy to interpret. This detector is referred to as symmetric plane detector or SPD. Second detector which should give real information about the background, at the sample position just after the end of the guide (Z = 164.4 m). This detector is referred to as endplane detector or EPD. Both of the detectors are planes spanning ±100 m in X and Y directions and utilize the Surface Source Write (SSW) [11, 21] functionality of MCNPX, which allows to obtain energy and position, among other parameters, of every neutron crossing the detector plane.

Note that apart from the statistical error present in the simulation, there is an expected 15 % systematic error associated with nuclear interaction models and nuclear data libraries when running simulations in MCNPX, which has been shown in [1].

4. The source

The neutron source for the simulations in this work has been modelled from running a full MCNPX simulation of the ESS target and moderator [19]. Further details on model of the source in this MCNPX model can be found in [20]. Neutrons that are produced in the process of spallation in the target arrive to the moderator and are slowed down. "The focusing" effect in MCNPX that attracts statistics has been used to boost statistics while sacrificing each particle's weight. To do this a circular area with radius of 12 cm has been specified to attract statistics. The choice of such an area is dictated by the approximate size of a neutron guide entrance, thus giving a boost to statistics of neutrons that enter the guide rather than focusing on monolith shielding, modelling which lies beyond the scope of this paper as mentioned earlier. Neutrons are then tracked back to the plane of the moderator surface and data on each neutron is written into a file for further use.

The ESS source covers a broad range of energies up to 3 GeV, which would mean that to simulate all the energy ranges to the same extent a long simulation is needed. To avoid having very long and complicated simulations we decided to take out some degree of complexity by simplifying the source. The position and angular distributions are left the same, while the energy distribution is changed to a fixed energy of 1 GeV. Check runs have been performed for energies of 1 MeV, 10 MeV, 100 MeV and 1 GeV. Their comparison showed that the simplified simulations preserve the all relevant physical effects and the only difference is the intensity. The reasoning is that the fastest neutrons, although few in number, are hardest to shield. Hence shielding efficiency against this radiation is likely to be even better for the lower energy neutrons. This is in greater detail explained in [20].

Choosing one energy for the emitted neutrons means that the detectors described in the previous section would detect neutrons that have either the energy of the source – 1 GeV or lower energies. The first case can occur when the neutron does not interact with any material and does not loose energy, thus being detected as emitted. In the other case, neutrons interact with matter, for example, via a spallation, neutron capture process or generating a shower [22], which leads to energy loss of the neutron and possibly also re-emission of secondary, lower energy neutrons.

Here we need to make one very important note: only neutrons coming from the moderator are considered. We cannot and are not making any statements considering the overall background, which most definitely needs to be explored in the near future, given the fact that during the time of this study the bunker design has been developing.

5. Runs with different thicknesses of steel shielding

This section describes our study of the thickness of the guide steel shielding. The steel shielding around the guide's substrate should act as shielding and this section presents the study of variations of the thickness of the shielding. Three thicknesses have been tested: 1 cm, 2 cm and 3 cm.

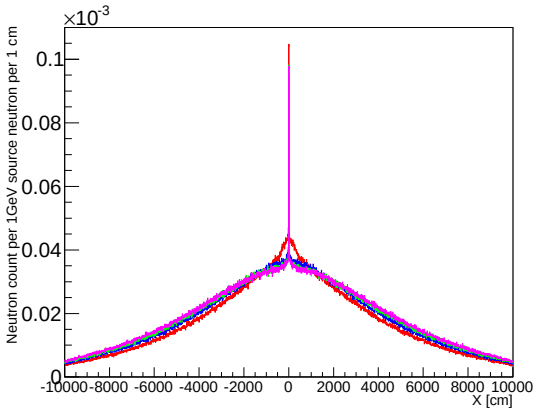

Figure 4. Neutron intensity projections on the X axis at the symmetric detector plane for three different steel shielding thicknesses around the guide. Red curve represents the run without steel shielding, blue – 1 cm of steel around the guide, green – 2 cm, magenta – 3 cm. The runs are made with 1 GeV neutron source.

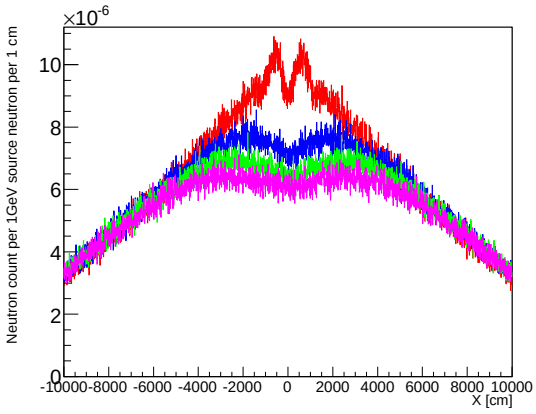

Figure 5. Neutron intensity projections on the X axis at the endplane detector for three different steel shielding thicknesses around the guide. Red curve represents the run without steel shielding, blue – 1 cm of steel around the guide, green – 2 cm, magenta – 3 cm. The runs are made with 1 GeV neutron source.

The results of these runs are presented in the form of intensity projections on the X axis and can be seen in figures 4 and 5. From the SPD plot in figure 4 one can see that the background level actually grows slightly in the region around the guide ($X < \pm 20$ m) with increasing steel thickness and gets even higher than the background solely from the substrate and coating, depicted in red. This can happen due to the presence of spallation in the model – having more material for the fast neutrons from the source to interact with also brings more secondary neutrons coming from spallation. Yet far away from the guide ($X > \pm 20$ m) the guide itself and it's close vicinity the background level falls with increasing thickness of the steel.

The background levels at the sample position (EPD) falls off with increased steel thickness. Two other very important observations are that, firstly, the background spreads in a wide range

and, secondly, the peak from the direct view of the moderator present in the SPD plot is gone at the sample position – EPD plot, which is the effect of going out of line-of-sight.

To get a better quantitative grasp of the situation at the sample position we resort to looking at the integrals under the intensity projections shown in figure 5. Since the integral values are a measure of how much the background level has dropped, this will help to compare the change in the different steel shielding thicknesses efficiencies via calculating a relative change with respect to the run with only substrate and coating, i.e. in the absence of the steel shielding whatsoever. The values are shown in table 1.

Table 1. Intensity integrals under the projection curves and relative change in integral value, calculated with respect to the model with only substrate and coating, for models with different steel thicknesses at the sample position (EPD).

Model	Integral	Relative change
Substrate+coating	0.01303±0.00004	n/a
1 cm steel	0.01213±0.00003	6.9±0.4 %
2 cm steel	0.01147±0.00003	12.0±0.4 %
3 cm steel	0.01095±0.00003	15.9±0.4 %

Judging from table 1 the increase in thickness from 1 cm to 2 cm gives almost a doubled increase in efficiency as compared to the change of solely adding a 1 cm steel shielding around the guide, going from 6.9±0.4 % to 12.0±0.4 %. Further increase of the thickness to 3 cm a slightly smaller increase of 3.9±0.6 %, suggesting that at 2 or 3 cm the effect is starting to decay slowly.

6. Runs with different steel wall thicknesses

Apart from adding a steel wall the rest of the model for these runs is unchanged and a 3 cm thick stainless steel shielding around the guide is used. Once again a simplified run with the source emitting only neutrons with energy of 1 GeV is used.

The results of the effect of the thickness of the stainless steel wall are presented as intensity projection on the X axis in figures 6 and 7. Compared to the plots in figures 4 and 5 we can clearly see that the background levels fall off in the region around the guide when the wall has been introduced into the model. Moreover there is a direct correlation with the walls thickness – the bigger the thickness, the lower the background drop.

A more quantitative representation of the date in the plots are the integrals under the curves, which are presented in table 2. From this, as well as from the plots, we can see that addition of even of a 0.5 m wall introduces a noticeable drop in background, which corresponds to 13.5±0.4 % relative change in background at sample position. Doubling the thickness to 1 m increases the relative change even more but to a smaller extent giving 19.5±0.4 %. Doubling the thickness once more to 2 m gives an increase but only by 1.3±0.6 % increasing the relative change to 20.8±0.4 %. From this we can conclude that a 1 m wall is the one that performs the most efficiently as compared to the additional price for a thicker wall.

7. Runs with different thicknesses of the polyethylene

We cover the guide with a layer of polyethylene (PE). This is a conventional material that is used for shielding purposes to moderate and scatter high energy neutrons, due to its high hydrogen content. The material that absorbs neutrons in this case is boron carbide (B_4C) in form of two 5 mm layers as mentioned above. The runs were performed with three different thicknesses of

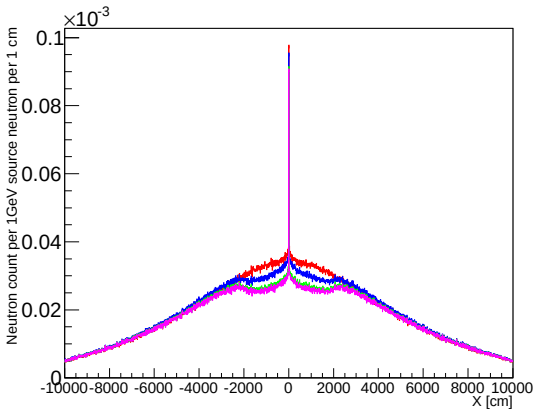

Figure 6. Neutron intensity projections on the X axis at the symmetric detector plane for three different steel wall thicknesses. 3 cm thick stainless steel shielding is used in the model. Red curve represents the run without the steel wall, blue – 0.5 m thick wall, green – 1 m thick, magenta – 2 m thick. The runs are made with 1 GeV neutron source.

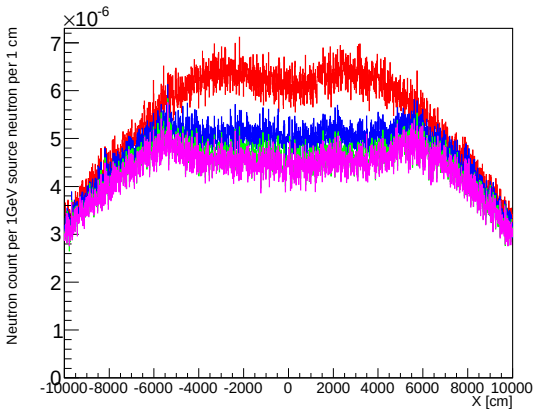

Figure 7. Neutron intensity projections on the X axis at the endplane detector for three different steel wall thicknesses. 3 cm thick stainless steel shielding is used in the model. Red curve represents the run without the steel wall, blue – 0.5 m thick wal, green – 1 m thick, magenta – 2 m thick. The runs are made with 1 GeV neutron source.

Table 2. Intensity integrals under the projection curves and relative change in integral value, calculated in respect to the model with 3 cm of steel shielding around the guide, for models with different wall thicknesses at the sample position (EPD).

Model	Integral	Relative change
3 cm steel	0.01095±0.00003	n/a
0.5 m wall	0.00948±0.00003	13.5±0.4 %
1 m wall	0.00882±0.00003	19.5±0.4 %
2 m wall	0.00867±0.00003	20.8±0.4 %

20 cm, 30 cm and 40 cm. The rest of the model is the same as described above, combining a 3 cm stainless steel shielding around and a 1 m thick, 10 m radius steel wall at position Z = 38 m. The runs are made with a simplified 1 GeV neutron source.

The results of such runs are presented in figures 8 and 9. As compared to the run of the model without any shielding, i.e. only substrate and coating, the background level has dropped significantly. Once again we see that there is a direct correlation between the thickness of the PE layer and the efficiency of the layer – the thicker the layer, the greater the efficiency at both SPD and EPD. From the plots we can also see that a 20 cm thick layer of borated PE (5 wt% B) works almost as efficient as a 20 cm thick PE layer combined with two 5 mm B_4C layers.

A more quantitative picture can be seen by looking at the integral values and relative changes of the integral values underneath the curves and this data is presented in table 3. We can see that the relative change by adding PE layer, 3 cm of shielding around the guide and a 1 m thick stainless steel wall is quite big – 75.9±0.4 %. Increasing the thickness of the PE layer by another 10 cm we get an increase of about 6.2±0.6 %. Another step in increasing the thickness by yet another 10 cm, making the PE layer 40 cm thick, gives only a minor 4.2±0.6 % increase.

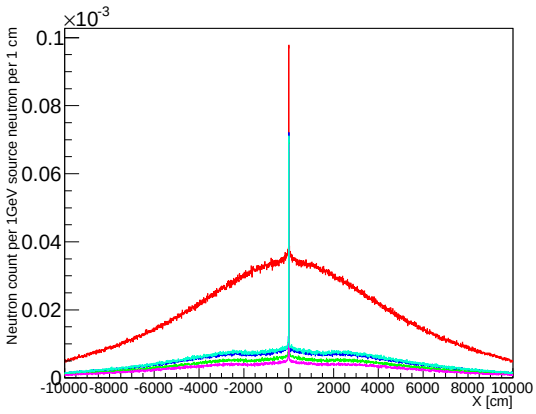

Figure 8. Neutron intensity projections on the X axis at the symmetric detector plane for three different polyethylene layer thicknesses. Red curve represents the run only with 3 cm of steel shielding around the guide, blue – with 3 cm of steel shielding around the guide, 1 m thick wall, 20 cm thick layer of polyethylene and two 5 mm thick layers of B_4C, green – the same as blue but with 30 cm thick layer of polyethylene, magenta – the same as blue but with 40 cm thick layer of polyethylene, cyan – the model which only has 20 cm thick layer of borated polyethylene (5 wt% Boron) around the guide without boron carbide layers. The runs are made with 1 GeV neutron source.

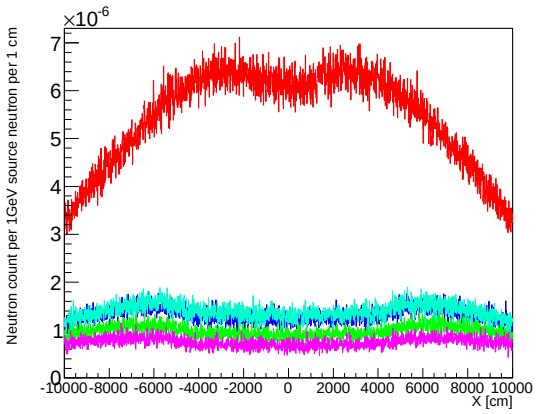

Figure 9. Neutron intensity projections on the X axis at the endplane detector for three different polyethylene layer thicknesses. Red curve represents the run only with 3 cm of steel shielding around the guide, blue – with 3 cm of steel shielding around the guide, 1 m thick wall, 20 cm thick layer of polyethylene and two 5 mm thick layers of B_4C, green – the same as blue but with 30 cm thick layer of polyethylene, magenta – the same as blue but with 40 cm thick layer of polyethylene, cyan – the model which only has 20 cm thick layer of borated polyethylene (5 wt% Boron) around the guide without boron carbide layers. The runs are made with 1 GeV neutron source.

Table 3. Intensity integrals under the projection curves and relative change in integral value, calculated in respect to the model with 3 cm of steel shielding around the guide, for models with 3 cm of steel shielding, 1 m thick steel wall, two B_4C layers and with different PE layer thicknesses at the sample position (EPD).

Model	Integral	Relative change
3 cm steel	0.01095±0.00003	n/a
20 cm PE layer	0.00264±0.00002	75.9±0.4 %
30 cm PE layer	0.00196±0.00001	82.1±0.4 %
40 cm PE layer	0.00150±0.00001	86.3±0.4 %
20 cm borated PE layer	0.00279±0.00002	74.5±0.4 %

From this we can conclude that the most reasonable thicknesses to use range between 20 cm and 30 cm. Using an expensive 20 cm borated polyethylene layer gives the same efficiency as the use of PE layer combined with two boron carbide layers, suggesting it is not the best material of choice.

For the model, described in this paper we decided to use a 20 cm, which reduces the total background level in a 1 GeV run from $(1.3\pm0.1)\cdot10^{-3}$ neutrons per cm^2 per 1 GeV source neutron

in model without the shielding to $(2.6\pm0.5)\cdot10^{-4}$ neutrons per cm^2 per 1 GeV source neutron for the model with full shielding setup as described in this section.

8. Comparison of neutron spectra at sample position.

After having investigated the effectiveness of various shielding parts and their configurations in the simplified 1 GeV runs it is very important to perform the run with a full ESS spectrum. Having obtained the data we want to compare the neutron spectra at the sample position for various setups, namely: the model with only supermirror coating and substrate, model with steel shielding around the guide, the final model with shielding around the guide, PE, B_4C and the wall and some kind of benchmark. The benchmark chosen is the cosmic neutron rate at sea level. The idea behind comparing neutron spectra at the sample position to the spectrum of the cosmic neutrons at sea level is the cosmic neutron background defines an order of magnitude of the lowest obtainable background in the instruments. This cosmic neutron spectra is roughly sketched in figure 10 with a black line and is taken from [23].

As mentioned earlier in the text, only neutrons coming from the moderator are considered and we cannot and are not making any statements considering the overall background, which most definitely needs to be explored in the near future, given the fact that during the time of this study the bunker design has been developing.

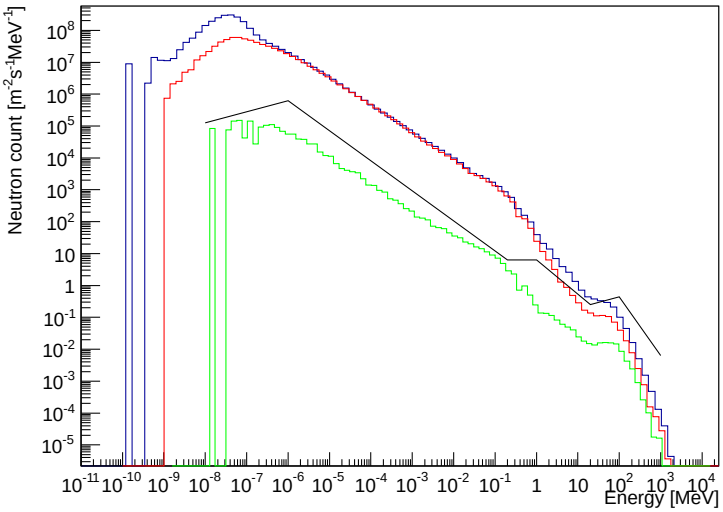

Figure 10. Neutron spectra comparison at the sample position, simulated with the full ESS neutron spectrum. Blue represents the model with only supermirror coating and substrate, red – the model with 3 cm of steel shielding around the guide, green – the final model with 3 cm of steel shielding and 20 cm PE layer around the guide, two 5 mm layers of boron carbide and the steel wall. The black line is a sketch of the cosmic neutron spectra at sea level, taken from [23].

From the plot in figure 10 we can see that the background without any shielding, just with supermirror coating and substrate (blue) is two orders of magnitude above the cosmic neutron rate, which does not satisfy requirements for detector operation. Having added 3 cm of steel shielding around the guide (red) we observe that some part of fast neutron intensities in energy range 10 – 100 MeV are cut down, which also leads to decrease in the amount of neutrons in thermal range ≈10 meV, presumably, due to the fact that there are less fast neutrons to induce secondary neutron emission.

Adding a 1 m thick, 10 m radius steel wall at position Z = 38 m to shield fast neutrons that get through the initial shielding, 20 cm thick layer of polyethylene to moderate fast neutrons and two 5 mm thick layers of boron carbide to absorb slowed down neutrons we move to the green curve. This curve goes below the black one in a broad energy range. Most important being the cold and thermal range – these are the neutrons that get scattered and detected in the experiments. More quantitatively the total background level has dropped from $(4.4\pm0.3)\cdot10^5$ cm^{-2}s^{-1} to $(2.7\pm0.2)\cdot10^3$ cm^{-2}s^{-1}, which is a significant two orders of magnitude drop.

9. Conclusion

In this paper a shielding model against fast and thermal/cold neutrons for the 162 m long guide system of the BIFROST spectrometer at ESS has been proposed and tested using MCNPX. Only neutrons coming from the moderator have been considered. The BIFROST neutron guide is modelled using the metal-substrate sandwich technology, which has its roots in MIRROTRON's metal-glass sandwich neutron guide construction technology.

Different parts of the shielding model have been tested for their efficiency in a simplified mode with source neutrons having a fixed energy of 1 GeV, namely: three different thicknesses of steel shielding around the guide, three different thicknesses of the steel wall and three different thicknesses of polyethylene layers surrounding the steel shielding of the guide.

After the simplified runs the model with chosen thicknesses of the above mentioned parts was tested with the full ESS spectrum and the results have shown that the background level drops below the cosmic neutron rate at sea level in a broad range of energies, most importantly in the cold and thermal ranges, since neutrons of these energies are the ones being scattered by the sample and detected by the detectors.

Acknowledgements

We than Stuart Ansell for many illuminating discussions and Jonas Okkels Birk for providing the initial model of the BIFROST guide system.

References

[1] Peggs S *et al* 2013 *ESS Technical Design Report* ESS 2013-001 **10** 20
[2] Cherkashyna N, DiJulio D D, Panzner T, Rantsiou E, Filges U, Ehlers G and Bentley P M 2015 *Phys. Rev.* ST Accel. Beams **18**
[3] Webpage www.mcstas.org
[4] Lefmann K and Nielsen N 1999 *Neutron News* **10** 20
[5] Willendrup P, Farhi E and Lefmann K 2004 *Physica* B **350** 735
[6] Willendrup P K, Knudsen E B, Klinkby E B, Nielsen T, Farhi E, Filges U and Lefmann K 2014 *J. Phys.: Conf. Series* **528**
[7] Willendrup P, Farhi E, Knudsen E B, Filges U and Lefmann K 2014 *Journal of Neutron Research* **17** issue 1 pp 35 - 43
[8] Waters L S *et al* 2007 *The MCNPX Monte Carlo radiation transport code* AIP Conf.Proc. **896** pp 81-90
[9] X-5 Monte Carlo Team 1987 MCNP – A General Monte Carlo N-Particle Transport Code, Version 5, *LA-UR-03-1987*
[10] Bertelsen M 2014 *Optimizing neutron guides using the minimalist principle and guide_bot* University of Copenhagen
[11] Klinkby E B *et al* 2013 Interfacing MCNPX and McStas for simulations of neutron transport *Nuclear Instruments & Methods in Physics Research* A **700**
[12] Klinkby E B, Knudsen E B, Willendrup P K, Lauritzen B, Nobœl E, Bentley P, Filges U 2014 Application of the MCNPX-McStas interface for shielding calculations and guide design at ESS *J. Phys.: Conf. Series* **528**
[13] Webpage http://europeanspallationsource.se/cluster *DMSC*
[14] Freeman P G *et al* 2015 CAMEA ESS - The continuous angle multi-energy analysis indirect geometry spectrometer for the european spallation source *Phys. Web of Conf.* **83**
[15] Birk J O, Marko M, Freeman P G, Jacobsen J, Hansen R L, Christensen N B, Niedermayer C, Månsson M, Rønnow H M, Lefmann K 2014 Prismatic analyser concept for neutron spectrometers *Rev. Sci. Instr.* **85**

[16] Bertelsen M, Jacobsen H, Hansen U B, Carlsen H H, Lefmann K 2013 Prismatic analyzer concept for neutron spectrometers *Nuclear Instruments & Methods in Physics Research* A **85**
[17] Webpage 2006 http://www.mirrotron.hu/media/Brosh/Brosh10.pdf *MIRROTRON*
[18] Cherkashyna N *et al* 2015 *Overcoming High Energy Backgrounds at Pulsed Spallation Sources* Proceedings of ICANS XXI
[19] Batkov K, Takibayev A, Zanini L and Mezei F 2013 Unperturbed moderator brightness in pulsed neutron sources *Nuclear Instr. Meth.* A **729**
[20] Mantulnikovs K 2015 *Neutron guide shielding for the BIFROST spectrometer at ESS* University of Copenhagen
[21] Knudsen E B, Klinkby E B and Willendrup P K 2014 McStas event logger: Definition and applications *Nuclear Instruments and Methods in Physics Research* Section A: Accelerators, Spectrometers, Detectors and Associated Equipment **738** pp 20 - 24
[22] Cherkashyna N *et al* 2014 High energy particle background at neutron spallation sources and possible solutions *J. Phys.: Conf. Series* **528**
[23] Hagmann C, Lange D and Wright D 2012 Monte carlo simulation of proton-induced cosmic-ray cascades in the atmosphere *Lawrence Livermore National Laboratory*